International Journal of Multiphase Flow 57 (2013) 102–114

Contents lists available at ScienceDirect

International Journal of Multiphase Flow

journal homepage: www.elsevier.com/locate/ijmulflow

A scaling analysis of added-mass and history forces and their coupling in dispersed multiphase flows

Y. Ling *, M. Parmar, S. Balachandar

Department of Mechanical and Aerospace Engineering, University of Florida, Gainesville, FL 32611, United States

ARTICLE INFO

Article history:
Received 11 April 2013
Received in revised form 19 June 2013
Accepted 27 July 2013
Available online 6 August 2013

Keywords:
Multiphase flows
Added-mass force
History force
Turbulent flows
Shock-particle interaction

ABSTRACT

Accurate momentum coupling model is vital to simulation of dispersed multiphase flows. The overall force exerted on a particle is divided into four physically meaningful contributions, *i.e.*, quasi-steady, stress-gradient, added-mass, and viscous-unsteady (history) forces. Time scale analysis on the turbulent multiphase flow and the viscous-unsteady kernel shows that the integral representation of the viscous-unsteady force is required except for a narrow range of particle size around the Kolmogorov length scale when particle-to-fluid density ratio is large. Conventionally, the particle-to-fluid density ratio is used to evaluate the relative importance of the unsteady forces (stress-gradient, added-mass, and history forces) in the momentum coupling. However, it is shown from our analysis that when particle-to-fluid density ratio is large, the importance of the unsteady forces depends on the particle-to-fluid length scale ratio and not on the density ratio. Provided the particle size is comparable to the smallest fluid length scale (*i.e.*, Kolmogorov length scale for turbulence or shock thickness for shock-particle interaction) or larger, unsteady forces are important in evaluating the particle motion. Furthermore, the particle mass loading is often used to estimate the importance of the back effect of particles on the fluid. An improved estimate of backward coupling for each force contribution is established through a scaling argument. The back effects of stress-gradient and added-mass forces depend on particle volume fraction. For large particle-to-fluid density ratio, the importance of the quasi-steady force in backward coupling depends on the particle mass fraction; while that of the viscous-unsteady force is related to both particle mass and volume fractions.

Published by Elsevier Ltd.

1. Introduction

Modeling and simulation have become important approaches to investigate multiphase flows in engineering and environmental applications. The multiphase flows of interest here are the so-called dispersed multiphase flows, which are characterized by a dispersed phase that is distributed in a carrier phase in the form of particles, droplets, and bubbles (see Balachandar and Eaton, 2010). Examples include particle suspension in gas or liquid flows, droplet dispersion in gas flows, and bubbly flows. As can be seen in these examples, the dispersed phase can be solid, liquid, or gas; while the carrier phase can be liquid or gas. In some extreme cases, such as heterogeneous explosive detonation, the carrier phase can be solid as well (see Ling et al., 2013). For simplicity, here after we refer to the dispersed and carrier phases as "particle" and "fluid", but it should be noted that the terms "particle" and "fluid" are used in a broad sense.

In typical applications, a very large number of particles are involved and the scales of primary interest are much larger than the size of an individual particle. Therefore, it is impractical to resolve the flow details at the particle scale. Instead, the point-particle approach (PPA) is commonly used, where particles are modeled as point masses. Since the flows around the particles are not resolved, the momentum and energy coupling between fluid and particles need to be given by proper models. In the incompressible regime, Maxey and Riley (1983) and Gatignol (1983) have derived rigorous expressions for the force on a particle undergoing arbitrary time-dependent motion in an unsteady inhomogeneous ambient flow. The overall interphase coupling force can be separated into different physically meaningful contributions: the quasi-steady force $\mathbf{F}_{qs}$, the stress-gradient force $\mathbf{F}_{sg}$, the added-mass force $\mathbf{F}_{am}$, and the viscous-unsteady force $\mathbf{F}_{vu}$ (often called the Basset history force). The latter three contributions together are loosely referred as the "unsteady forces", since they are non-zero only when the acceleration of the fluid or the particle is non-zero. The Maxey-Riley-Gatignol (MRG) equation of motion has also been

* Corresponding author. Current address: Institut Jean Le Rond d'Alembert, Université Pierre et Marie Curie, 4, Place Jussieu 75252 Paris Cedex 05, France. Tel: +33 (0)1 44 27 87 14.
E-mail address: yueling@dalembert.upmc.fr (Y. Ling).

0301-9322/$ - see front matter Published by Elsevier Ltd.
http://dx.doi.org/10.1016/j.ijmultiphaseflow.2013.07.005

extended to compressible flows recently by Parmar et al. (2011, 2012). The above theoretical formulations are asymptotically valid in the limit of small Reynolds and Mach numbers, but they serve as theoretical basis for empirical extension to finite Reynolds and Mach numbers.

At the level of an isolated particle in an incompressible flow, the importance of the unsteady forces compared to the quasi-steady force has been investigated by Bagchi and Balachandar (2002). Their scaling analysis showed that the ratios $|\mathbf{F}_{am}/\mathbf{F}_{qs}|$ and $|\mathbf{F}_{vu}/\mathbf{F}_{qs}|$ scale as $1/(\rho_p/\rho_f + C_M)$ and $1/\sqrt{(\rho_p/\rho_f + C_M)}$, respectively, if unsteadiness is due to particle acceleration. Here ρ_p and ρ_f are the densities of the particle and the fluid, and C_M is the added-mass coefficient. This scaling is in complete agreement with conventional expectation that in case of a particle much heavier than the fluid (*i.e.*, $\rho_p/\rho_f \gg 1$) unsteady forces are small compared to the quasi-steady force and can be ignored. This is the reason why added-mass and other unsteady forces are included in the simulations of bubbly flows (see Pougatch et al., 2008) and liquid–solid flows (see Snider et al., 1998; Patankar and Joseph, 2001) but often ignored in the context of gas-particle flows. However, this conclusion is not valid in case of unsteady effects arising from fluid acceleration. While the magnitude of particle acceleration is controlled by the particle mass, there is no such limitation to the magnitude of the ambient fluid acceleration seen by the particle. As a result, in case of fluid acceleration, Bagchi and Balachandar (2002) showed $|\mathbf{F}_{sg}/\mathbf{F}_{qs}|$ and $|\mathbf{F}_{am}/\mathbf{F}_{qs}|$ to scale as $\mathrm{Re}_p(d_p/L)$ and $|\mathbf{F}_{vu}/\mathbf{F}_{qs}|$ to scale as $\sqrt{\mathrm{Re}_p(d_p/L)}$, where Re_p is particle Reynolds number based on particle diameter (d_p) and relative velocity, and L is length scale of the ambient flow. Clearly, these ratios can be large even in case of heavier-than-fluid particles and thus when fluid acceleration is strong it may be necessary to include the unsteady forces even in case of gas–solid flows.

This situation is particularly relevant in compressible flows, where shocks and other discontinuities, as they pass over a particle, contribute to rapid variation in the ambient flow seen by the particle, see Parmar et al. (2009). The resulting unsteady force contributions arising from shock-particle interaction was systematically investigated by Ling et al. (2011a,b). Their primary conclusion was that as the shock moves over a particle the unsteady forces due to ambient fluid acceleration are an order of magnitude or more larger than the quasi-steady force. Furthermore, as can be expected from the scaling analysis of Bagchi and Balachandar (2002), the magnitude of the enhanced unsteady forces is independent of the particle-to-fluid density ratio (*i.e.*, even in case of gas–solid flows unsteady forces are large when a shock passes over the particle). However, the duration of this strong unsteady contribution is limited to only a brief period as the shock passes over the particle. Therefore, the integrated effect of the unsteady force contributions ($\mathbf{F}_{sg}$, $\mathbf{F}_{am}$ and $\mathbf{F}_{vu}$) on the long-term post-shock motion of the particle may not necessarily be significant. In terms of contribution to the long-term post-shock particle velocity, the role of unsteady force contributions was observed to be important only in case of $\rho_p/\rho_f \sim O(1)$.

The above investigations have generally been in the context of an isolated particle. As a result, they are applicable for dilute multiphase flows, where the influence of particles on the macroscale fluid motion is negligibly small. Under such dilute condition the fluid-particle interaction can be considered one-way coupled. In other words, the particle motion is dictated by the fluid flow, but the particles do not influence the fluid flow. However, in many applications, where the mass loading of particles is finite, the influence of particles on the macroscale fluid flow is significant. Then the fluid and particles are two-way coupled, see Crowe et al. (1998); Balachandar and Eaton (2010); Subramaniam (2013). In the literature, the effect of fluid on particles is usually referred as forward coupling; while the reverse effect of particles on fluid is referred backward coupling, see Garg et al. (2007) and Ling et al. (2010).

Here we are interested in multiphase flow problems where both two-way coupling and unsteady mechanisms are of importance. In this flow regime we are interested in addressing the following three fundamental questions on interphase coupling:

- Q1: *Is it possible to simplify the history integral in computing viscous-unsteady force? If so, under what conditions can this simplification be made?*
- Q2: *Under what conditions are unsteady forces important in evaluating the particle motion when compared to quasi-steady force?*
- Q3: *Under what conditions does the back effect of both quasi-steady and unsteady forces need to be taken into account in the fluid momentum equation, (i.e., under what conditions the fluid and particles are considered as two-way coupled)?*

For Q1, the viscous-unsteady force is generally computed as the Basset-like convolution integral of the past history of the relative acceleration between the particle and the surrounding fluid weighted by the history kernel. The evaluation of this convolution integral is computationally very costly. However, if the rate of change of the relative acceleration is slower than the decay of the kernel then the convolution integral can be simplified and pre-computed. In this paper, by investigating the time scale of the viscous-unsteady kernel in relation to the turbulence time scale, we will establish the condition under which the convolution integral can be simplified.

For Q2, the particle-to-fluid density ratio, ρ_p/ρ_f, is conventionally used in evaluating the importance of the unsteady forces. Based on this argument, unsteady forces are often neglected in gas-particle flows, where $\rho_p/\rho_f \gg 1$. However, the scaling analysis of the unsteady forces by Bagchi and Balachandar (2002) has shown that the conventional criterion is proper in case of unsteady forces arising from particle acceleration, but must be modified if the added-mass and viscous-unsteady forces are due to fluid acceleration. Here we will extend this analysis with a more rigorous evaluation of the particle response to a range of turbulent scales. In particular, we will follow the approach of Balachandar (2009) to obtain the scales of relative velocity and relative acceleration seen by the particle in the three regimes characterized by $\tau_p < \tau_\eta$, $\tau_\eta < \tau_p < \tau_L$, and $\tau_L < \tau_p$, where τ_p is the particle response time, τ_η and τ_L are the Kolmogorov and integral time scales of the ambient flow (precise definitions of the time scales will be given in Section 3). From these characteristic scales, quantitative estimates of the relative importance of the unsteady forces in a turbulent flow will be obtained.

For Q3, the particle mass fraction ratio, defined as the mass ratio between the particles and fluid in a unit volume of the multiphase flow, is usually taken as the momentum coupling parameter, see Crowe et al. (1998). The general rule of thumb is that when the momentum coupling parameter is $O(1)$ or more, the fluid and particles are two-way coupled. This conventional momentum coupling parameter considers only the quasi-steady component of the backward coupling force, and thus may not apply when unsteady forces dominate interphase coupling. Here we will present a scaling argument to establish conditions under which quasi-steady and unsteady forces must be included in the backward momentum coupling. It should be reminded that when the volume fraction of particles is finite, the evolution of the which can also significantly influence the fluid flow through the fluid continuity equation (Eq. (1)). Nevertheless, the present paper focuses only on dilute flows where the influence of the particles on the fluid flow is only through momentum transfer.

To simplify and focus the discussion to answering the three questions in the context of particle-turbulence interaction, the present scaling analysis ignores the effect of gravity. Hence, the results to be presented below and the conclusions to be drawn are strictly valid only in the limit gravity and gravity-induced settling of particles plays a minor role. The effects of gravitational settling on relative velocity and particle Reynolds number have been addressed by Balachandar (2009). Following along that line of reasoning, the present scaling analysis can be extended to incorporate the effect of gravity. Another important limitation of the present analysis is that the particle velocity is assumed to be entirely dictated by the fluid flow. In other words, we assume that the effect of particle initial conditions (such as particle injection velocity) have been forgotten and not of importance in the scaling analysis. This assumption is appropriate if the residence time of the particles within the system is much larger than the particle time scale. There are applications where this assumption is violated. In such cases, the injection velocity (or the initial conditions) will play an important role and the present scaling analysis must be re-evaluated with appropriate estimates of the different forces.

In pursuit of these goals, we first briefly describe the governing equations for both the continuous and dispersed phases and the model for the interphase coupling forces in Section 2. We then present a general analysis of particle time scale, relative velocity and relative acceleration between the fluid and particles in Section 3. Discussions about the integral and non-integral representations of viscous-unsteady force are presented in Section 4. A scaling analysis is conducted to evaluate the importance of the unsteady forces in forward momentum coupling in Section 5. Similarly, in Section 6, we investigate the importance of the contribution of each interphase coupling force in backward momentum coupling and establish improved estimates for the momentum coupling parameters for each force. Finally, conclusions are drawn in Section 7.

2. Governing equations

2.1. Point-particle approach (PPA)

The point-particle approach is a useful method in the computations of dispersed multiphase flows, including inviscid (see Ling et al., 2011b) and viscous (turbulent) flows (see Squires and Eaton, 1991; Elghobashi and Truesdell, 1992), incompressible (see Andrews and O'Rourke, 1996; Snider et al., 1998) and compressible flows (see Balakrishnan et al., 2010; Ling et al., 2012). Here we pursue the PPA formulated under the Eulerian–Lagrangian framework: the fluid is viewed as continuum and the governing equations are written in the Eulerian framework; while the particles are retained as discrete point masses and tracked in the Lagrangian framework. In this paper, we focus on the momentum coupling between fluid and particles, and thus the energy equations of both fluid and particles are not considered. The governing equations for fluid and particles are given as

$$\frac{\partial(\rho_f\phi_f)}{\partial t}+\nabla\cdot(\rho_f\phi_f\mathbf{u}_f)=0, \tag{1}$$

$$\rho_f\phi_f\frac{D\mathbf{u}_f}{Dt}-\nabla\cdot\boldsymbol{\sigma}_f=-\frac{1}{\mathbb{V}}\sum_i\mathbf{F}_{fp,i}, \tag{2}$$

and

$$\frac{d\mathbf{x}_{p,i}}{dt}=\mathbf{u}_{p,i}, \tag{3}$$

$$m_{p,i}\frac{d\mathbf{u}_{p,i}}{dt}=\mathbf{F}_{fp,i}, \tag{4}$$

The subscripts f and p denote properties associated with the fluid and particles, respectively. The fluid variables, ρ_f and ϕ_f, represent the density and volume fraction of fluid. The bold symbols $\mathbf{u}_f$ and $\boldsymbol{\sigma}_f$ represent the velocity vector and stress tensor of fluid.

The position and velocity vectors, and the mass of the ith particle are denoted by $\mathbf{x}_{p,i}$, $\mathbf{u}_{p,i}$, and $m_{p,i}$. The overall force on the i^{th} particle due to fluid-particle interaction is denoted by $\mathbf{F}_{fp,i}$. In PPA, as the flow around particles is not resolved, the expression of $\mathbf{F}_{fp,i}$ is given by fluid-particles coupling models in terms of the macroscale (undisturbed) fluid flow properties. Due to Newton's third law, $\mathbf{F}_{fp,i}$ needs to be subtracted from the fluid momentum equation (Eq. (2)) to account for the back effect of the particles on the fluid flow. In Eq. (2), $\sum_i$ represents sum over all the particles within the cell and $\mathbb{V}$ denotes the cell volume.

In forward momentum coupling (solving Eqs. (3) and (4)), the fluid quantities at the particle location need to be evaluated through interpolation from fluid solutions in neighboring cell centers or grid points. In backward coupling, the force exerted on a particle needs to be projected back to the fluid solution at neighboring cell centers, *i.e.*, the term $-\frac{1}{\mathbb{V}}\sum_i\mathbf{F}_{fp,i}$ appearing in Eq. (2) must be distributed to the cell volume or to the surrounding grid points. More discussions on numerical issues pertaining to forward and backward coupling can be found in Crowe (1982), Squires and Eaton (1990), Sundaram and Collins (1996), Snider (2001), Garg et al. (2007), and Ling et al. (2010).

At last, it should be mentioned that when particle volume fraction is significantly high, particle–particle interaction becomes important. As a result, there will be additional force that must be added to the RHS of Eq. (4), see Andrews and O'Rourke (1996), Snider et al. (1998), Ling et al. (2011a). However, as the focus of this paper is on fluid-particle coupling, we ignore the contribution of particle–particle interaction to force. Note that this simplification will not influence the analysis given below.

2.2. Interphase coupling force formulations

The overall interphase coupling force exerted on a particle can be divided into different physically meaningful contributions. This linear superposition can be rigorously established in the limit of zero Reynolds and Mach numbers for an isolated particle, see Maxey and Riley (1983), Parmar et al. (2011, 2012). Nevertheless, it provides a theoretical basis for empirical extensions to finite Reynolds and Mach numbers and particle volume fraction. Such empirical extensions have been proposed in many previous works, comprehensive reviews of which can be found in Magnaudet and Eames (2000) and Ling et al. (2011a, 2012) for incompressible and compressible flows.

For an individual particle, the particle equation of motion, Eq. (4), can be written as

$$m_p\frac{d\mathbf{u}_p}{dt}=\mathbf{F}_{fp}=\mathbf{F}_{qs}+\mathbf{F}_{sg}+\mathbf{F}_{am}+\mathbf{F}_{vu}, \tag{5}$$

where $\mathbf{F}_{qs}$, $\mathbf{F}_{sg}$, $\mathbf{F}_{am}$, and $\mathbf{F}_{vu}$ represent the quasi-steady, stress-gradient, added-mass, and viscous-unsteady forces, the expressions of which are given as

$$\mathbf{F}_{qs}=3\pi\mu d_p(\mathbf{u}_f-\mathbf{u}_p)\Phi(\mathrm{Re}_p), \tag{6}$$

$$\mathbf{F}_{sg}=V_p\rho_f\frac{D\mathbf{u}_f}{Dt}, \tag{7}$$

$$\mathbf{F}_{am}=V_pC_M\left(\frac{D\rho_f\mathbf{u}_f}{Dt}-\frac{d\rho_f\mathbf{u}_p}{dt}\right), \tag{8}$$

$$\mathbf{F}_{vu}=\frac{3}{2}d_p^2\sqrt{\pi\nu}\sqrt{\tau_{vu}}\int_{-\infty}^{t}K_{vu}\left(\frac{t-\xi}{\tau_{vu}},\mathrm{Re}_p\right)\left(\frac{D\rho_f\mathbf{u}_f}{Dt}-\frac{d\rho_f\mathbf{u}_p}{dt}\right)\frac{d\xi}{\tau_{vu}}, \tag{9}$$

where V_p denotes the particle volume, μ and ν represent the dynamic and kinematic viscosity of the fluid. The added-mass coefficient is denoted by C_M, which is taken to be 1/2. The correction function that accounts for the effect of finite Reynolds number on

the quasi-steady force is generally taken to be given as (see Clift et al., 1978)

$$\Phi(\mathrm{Re}_p) = 1.0 + 0.15\mathrm{Re}_p^{0.687}. \tag{10}$$

The definition of Re_p is given as

$$\mathrm{Re}_p = \frac{|\mathbf{u}_f - \mathbf{u}_p| d_p}{\nu}. \tag{11}$$

The viscous unsteady kernel, K_{vu}, is defined as a function of normalized time scaled by the viscous-unsteady time scale, *i.e.*, τ_{vu}. More discussions about the viscous unsteady force and the corresponding time scale will be presented in Section 4.

Note that in the above force expressions, the fluid density is taken to be a variable and correctly retained within the derivatives. In addition, in compressible flows the quasi-steady correction function Φ, the added-mass coefficient C_M, and the viscous unsteady kernel K_{vu} will depend also on particle Mach number defined as

$$\mathrm{M}_p = \frac{|\mathbf{u}_f - \mathbf{u}_p|}{c_f}, \tag{12}$$

where c_f denotes the speed of sound of fluid, see Parmar et al. (2008) and Ling et al. (2012). Such complications do not alter the scaling arguments to be presented below and therefore will not be further addressed here. Furthermore, in problems such as shock-particle interaction, the added-mass force will also need to be expressed as a history integral. Implications of this integral representation will be discussed in Appendix A.

When particle volume fraction is finite, the quasi-steady force correction function Φ and the viscous-unsteady kernel K_{vu} will depend also on the particle volume fraction ϕ_p, see Sangani et al. (1991), Ling et al. (2012), and Subramaniam (2013). Since the present study focuses on developing the scaling estimates for the fluid-particle coupling, the effect of particle volume fraction is neglected to simplify the analysis.

3. General analysis of turbulent multiphase flows

3.1. Characteristic time scale for particle motion

In order to estimate the relative importance of the unsteady contributions to forward and backward momentum coupling, the first step is to establish the scaling of the relative velocity and relative acceleration between the fluid and particle. For the purpose of scaling, it is useful to define the time scale for particle motion.

It is customary to define the particle time scale as the time it takes for a particle instantaneously released in a uniform stream to accelerate and the relative velocity reach $(1/e)$ times the ambient uniform flow velocity. Under such simplified conditions, Eqs. (5)–(8) can be solved to define the time scale for particle motion as

$$\tau_p = \frac{d_p^2}{12\beta\nu}\frac{1}{\Phi(\mathrm{Re}_p)}, \tag{13}$$

where $\beta = 3/(2\rho_p/\rho_f + 1)$. For a heavy particle $\beta = 0$, for neutrally buoyant particles $\beta = 1$, and for bubbles, $\beta = 3$. In obtaining the above definition from Eq. (5), the effect of the history force (Eq. (9)) has been ignored. When $\mathrm{Re}_p$is finite, the non-linear effect to the quasi-steady force is incorporated by introducing the correction function $\Phi(\mathrm{Re}_p)$.

For a heavy particle, *i.e.*, $\rho_p/\rho_f \to \infty$, τ_p reduces to τ_p', where

$$\tau_p' = \frac{\rho_p/\rho_f d_p^2}{18\nu}\frac{1}{\Phi(\mathrm{Re}_p)}. \tag{14}$$

Note that τ_p' is conventionally defined as the particle response time, see Crowe et al. (1998).

For a bubble, *i.e.*, $\rho_p/\rho_f \to 0$,

$$\tau_p = \frac{d_p^2}{36\nu}\frac{1}{\Phi(\mathrm{Re}_p)}, \tag{15}$$

indicating that the acceleration of a bubble is dictated by the added-mass force.

3.2. Relative velocity and relative acceleration corresponding to l-size eddy in turbulent multiphase flows

Here, we will estimate the relative velocity and relative acceleration between the particle and the surrounding fluid, *i.e.*, $|\mathbf{u}_f - \mathbf{u}_p|$ and $|D\mathbf{u}_f/Dt - d\mathbf{u}_p/dt|$, in the context of turbulent multiphase flows.

In turbulent dispersed multiphase flows, a particle will interact with eddies of different sizes. The hypothesis made here is that, the particle will respond to an eddy of size l only when the time scale of the particle is smaller than that of the eddy, *i.e.*, $\tau_p < \tau_l$, where τ_l is the time scale of l-size eddy. In such a case, the relative velocity due to the l-size eddy can be obtained from equilibrium Eulerian approximation (see Ferry and Balachandar, 2001) which is given as

$$\mathbf{u}_f - \mathbf{u}_p = \tau_p(1-\beta)\frac{D\mathbf{u}_f}{Dt} + O\left(\tau_p^{3/2}\right). \tag{16}$$

The above equation is an asymptotic solution of the particle equation of motion (Eq. (4)) with the Stokes number as the small parameter. The Stokes number corresponding to l-size eddy is defined as

$$\mathrm{St}_l = \frac{\tau_p}{\tau_l}. \tag{17}$$

A simple interpretation of Eq. (16) is that under equilibrium particle motion, the relative velocity is dictated by particle's inability to respond to local fluid acceleration just as a fluid element. Extensive tests in isotropic and wall-bounded turbulent flows have shown that the leading term of the expansion (the first term of the right hand side of Eq. (16)) is sufficient to obtain accurate estimation of relative velocity for particles of $\mathrm{St}_l < 1$, see Ferry and Balachandar (2001) and Ferry et al. (2003). Furthermore, it can be easily shown that Eq. (16) with the higher order term ignored is equivalent to $d\mathbf{u}_p/dt = D\mathbf{u}_f/Dt$. The fluid acceleration of the l-size eddy can be approximated as $|D\mathbf{u}_f/Dt| \sim u_l/\tau_l$, where u_l is the velocity scale of the l-size eddy. Therefore, the equilibrium Eulerian approximation gives the following estimates of the relative velocity and relative acceleration for $\mathrm{St}_l < 1$ ($\tau_p < \tau_l$) as

$$\left.\begin{aligned} &|\mathbf{u}_f - \mathbf{u}_p|_l \approx \tau_p|1-\beta|\tfrac{u_l}{\tau_l}, \\ &\left|\tfrac{D\mathbf{u}_f}{Dt} - \tfrac{d\mathbf{u}_p}{dt}\right|_l \approx 0. \end{aligned}\right\} \quad \text{if } \mathrm{St}_l < 1. \tag{18}$$

In contrast, when $\tau_p > \tau_l$ ($\mathrm{St}_l > 1$), the particle is too sluggish to respond to the l-size eddy motion. Then the contribution to relative velocity from the l-size eddy will be dictated by eddy velocity instead of eddy acceleration. Also as the particle acceleration in response to such l-size eddy is negligible, the relative acceleration is dictated by the fluid acceleration alone. Therefore, relative velocity and relative acceleration can be approximated as

$$\left.\begin{aligned} &|\mathbf{u}_f - \mathbf{u}_p|_l \approx |1-\beta|u_l, \\ &\left|\tfrac{D\mathbf{u}_f}{Dt} - \tfrac{d\mathbf{u}_p}{dt}\right|_l \approx \tfrac{u_l}{\tau_l}. \end{aligned}\right\} \quad \text{if } \mathrm{St}_l > 1. \tag{19}$$

The above estimates are appropriate only for longtime particle behavior for times much larger than τ_p. In this limit, the particle motion is dictated by the surrounding turbulent flow and not by initial conditions, such as injection velocity. Furthermore, the above estimates ignore the effect of gravity and other external forces that may also control particle motion. Estimates of relative velocity

including the effect of gravity have been discussed by Balachandar (2009).

In turbulent flows, there exist eddies of size varying from Kolmogorov to integral length scales. The eddy velocity and time scales increase with the eddy size as $u_l \sim (\epsilon l)^{1/3}$ and $\tau_l \sim l^{2/3}/\epsilon^{1/3}$, where ϵ is the dissipation rate that is set by the energy containing large eddies and maintained through the inertial range. In contrast, the eddy acceleration, $(Du/Dt)_l = u_l/\tau_l \sim \epsilon^{2/3}/l^{1/3}$, decreases with eddy size. Therefore, in turbulent flows, the maximum fluid acceleration is dictated by the Kolmogorov eddy, while the maximum fluid velocity scale is represented by integral scale eddies.

The above turbulent scales along with the estimates of relative velocity given in Eqs. (18) and (19), can be used to estimate the particle Reynolds number corresponding to the l-size eddy as

$$\begin{cases} \mathrm{Re}_{p,l}\Phi(\mathrm{Re}_{p,l}) \approx \frac{|1-\beta|}{12\beta}\left(\frac{d_p}{\eta}\right)^3\left(\frac{\eta}{l}\right)^{1/3}, & \text{if } \mathrm{St}_l < 1, \\ \mathrm{Re}_{p,l} \approx |1-\beta|\left(\frac{d_p}{\eta}\right)\left(\frac{l}{\eta}\right)^{1/3}, & \text{if } \mathrm{St}_l > 1. \end{cases} \tag{20}$$

3.3. Different regimes in turbulent multiphase flows

In this section we will use the results of the previous section on the relative velocity and relative acceleration in response to a l-size eddy to obtain estimates of maximum relative velocity and particle Reynolds number for a particle subjected to a range of turbulent eddies.

Based on the value of particle time scale τ_p in relation to the range of fluid time scales from the Kolmogorov scale τ_η to the integral time scale τ_L, we can identify three different regimes of particle behavior as suggested by Balachandar (2009):

- Regime I Particles ($\tau_p < \tau_\eta$): In this regime, $\mathrm{St}_L < \mathrm{St}_\eta < 1$, where $\mathrm{St}_L = \tau_p/\tau_L$ and $\mathrm{St}_\eta = \tau_p/\tau_\eta$. Since τ_η is the smallest time scale in the fluid flow, the particle will respond to every eddy in the flow. Therefore, the relative velocity and relative acceleration corresponding to every eddy can be estimated by Eq. (18). Since relative velocity is dictated by eddy acceleration, $|\mathbf{u}_f - \mathbf{u}_p|$ decreases with the eddy time scale, as shown in Fig. 1(a). As the fluid acceleration of the Kolmogorov eddies is the largest, the maximum velocity difference in this regime is

$$|\mathbf{u}_f - \mathbf{u}_p|_{\max,\mathrm{I}} \approx \tau_p|1-\beta|\frac{u_\eta}{\tau_\eta}. \tag{21}$$

Similarly, the particle Reynolds number can be estimated by Eq. (20). The particle Reynolds number must be based on the maximum relative velocity between the particle and the turbulent flow and in this regime it is dictated by the Kolmogorov scale as

$$\mathrm{Re}_{p,\mathrm{I}}\Phi(\mathrm{Re}_{p,\mathrm{I}}) \approx \frac{|1-\beta|}{12\beta}\left(\frac{d_p}{\eta}\right)^3. \tag{22}$$

- Regime II Particles ($\tau_\eta < \tau_p < \tau_L$ or $\mathrm{St}_\eta < 1$): In this regime, $\mathrm{St}_L < 1 < \mathrm{St}_\eta$. The particle responds to the large eddies in the flow but not to the small ones. There exists an eddy of size l^* ($\eta < l^* < L$), whose time scale matches the particle time scale, *i.e.*, $\tau_{l^*} = \tau_p$. The particle will respond to the larger eddies with $\tau_l > \tau_{l^*}$, and the relative velocity and relative acceleration are represented by Eq. (18). On the other hand, the particle does not respond to the smaller eddies of $\tau_l < \tau_{l^*}$, and the relative velocity and relative acceleration are as given by Eq. (19). It can be shown from Eqs. (18) and (19) that, the relative velocity increases with τ_l for $\tau_l < \tau_{l^*}$ and decreases for $\tau_l > \tau_{l^*}$ (see Fig. 1(a)). The relative velocity reaches its maximum at τ_{l*}, whose value is given by

$$|\mathbf{u}_f - \mathbf{u}_p|_{\max,\mathrm{II}} \approx \tau_p|1-\beta|\frac{u_{l^*}}{\tau_{l^*}} = |1-\beta|u_{l^*}. \tag{23}$$

The particle Reynolds number based on the maximum relative velocity in this regime is

$$\mathrm{Re}_{p,\mathrm{II}}\sqrt{\Phi(\mathrm{Re}_{p,\mathrm{II}})} \approx \frac{|1-\beta|}{\sqrt{12\beta}}\left(\frac{d_p}{\eta}\right)^2. \tag{24}$$

- Regime III Particles ($\tau_p > \tau_L$): In this regime, $1 < \mathrm{St}_L < \mathrm{St}_\eta$. The particle time scale exceeds all the fluid time scales and thus the particle does not respond to any eddy. The relative velocity and relative acceleration are then given by the eddy velocity and acceleration as shown in Eq. (19). Since the largest fluid velocity scale is dictated by the integral velocity scale u_L, the maximum relative velocity in this regime can be approximated as

$$|\mathbf{u}_f - \mathbf{u}_p|_{\max,\mathrm{III}} \approx |1-\beta|u_L, \tag{25}$$

and the particle Reynolds number in this regime is

$$\mathrm{Re}_{p,\mathrm{III}} \approx |1-\beta|\left(\frac{d}{\eta}\right)\left(\frac{L}{\eta}\right)^{1/3}. \tag{26}$$

Fig. 1(a) shows a schematic of the contribution to relative velocity from the Kolmogorov to the integral scale eddies in the three different regimes. In each regime the largest contribution to rela-

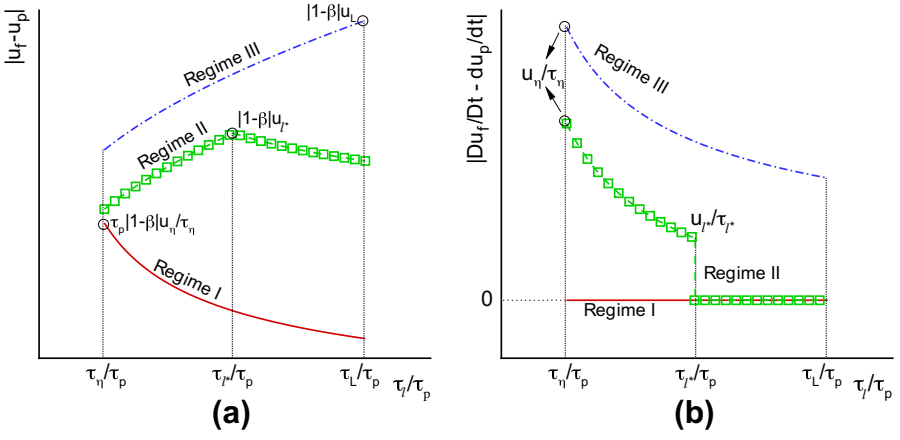

Fig. 1. Estimates of the relative (a) velocity and (b) acceleration between fluid and particle as functions of τ_l/τ_p for the three different regimes (Regime I: $\tau_p < \tau_\eta$; Regime II: $\tau_\eta < \tau_p < \tau_L$; Regime III: $\tau_p > \tau_L$).

tive velocity is marked as an open circle. The corresponding schematic for relative acceleration for the three different regimes is shown in Fig. 1(b). The maximum relative velocity and the particle Reynolds number in the three different regimes are consistent with those obtained by Balachandar (2009).

4. Integral representation of the viscous-unsteady force in turbulent multiphase flows

If the time scales of all the turbulent eddies are substantially larger than the time scale of viscous-unsteady kernel K_{vu}, then the relative acceleration $(D\rho_f\mathbf{u}_f/Dt - d\rho_f\mathbf{u}_p/dt)$ in Eq. (9) can be treated as a constant and the integral of the kernel can be precomputed. This approximation can lead to significant simplification of the viscous unsteady force formulation. In this section, using the time scales of turbulence and viscous-unsteady kernel along with the particle time scale, we obtain an estimate as to under what conditions the integral in Eq. (9) can be simplified.

For simplicity, we consider the viscous-unsteady kernel to be that given by Mei and Adrian (1992), which transits from the $t^{-1/2}$ decay at small times to a faster t^{-2} decay at large times. The viscous-unsteady time scale τ_{vu} can then be defined as the transition point from the slower to the faster decay of the kernel. Using the definition

$$\tau_{vu} = \frac{d_p^2}{\nu}\left(\frac{4}{\pi}\right)^{1/3}\left(\frac{0.75+0.105\mathrm{Re}_p}{\mathrm{Re}_p}\right)^2, \tag{27}$$

the viscous-unsteady kernel K_{vu} of Mei and Adrian (1992) can be expressed as

$$K_{vu}(t/\tau_{vu}) = \frac{1}{\left[(t/\tau_{vu})^{1/4} + t/\tau_{vu}\right]^2}, \tag{28}$$

which is plotted in Fig. 2. When $t \ll \tau_{vu}$, K_{vu} reduces to the Basset history kernel K_{BH} as

$$K_{vu}(t/\tau_{vu})|_{t\ll\tau_{vu}} \to K_{BH}(t/\tau_{vu}) = \frac{1}{\sqrt{t/\tau_{vu}}}; \tag{29}$$

when $t \gg \tau_{vu}$, K_{vu} will reach the non-linear limit K_{NL} as

$$K_{vu}(t/\tau_{vu})|_{t\gg\tau_{vu}} \to K_{NL}(t/\tau_{vu}) = \frac{1}{(t/\tau_{vu})^2}. \tag{30}$$

As shown in Fig. 2, K_{vu} changes from the $t^{-1/2}$ decay at short time to the faster t^{-2} decay at long time. Due to the fast decay for $t > \tau_{vu}$, if the particle and fluid acceleration time scales are much larger than τ_{vu}, then Eq. (9) can be reduced to the following simpler form

$$\mathbf{F}_{vu} = V_p C_{vu}\left(\frac{D\rho_f\mathbf{u}_f}{Dt} - \frac{d\rho_f\mathbf{u}_p}{dt}\right), \tag{31}$$

which is similar to the added-mass force. Here the effective viscous-unsteady coefficient C_{vu} is defined as

$$C_{vu} = \frac{9}{\sqrt{\pi}}\left(\frac{4}{\pi}\right)^{1/6}\left(\frac{0.75+0.105\mathrm{Re}_p}{\mathrm{Re}_p}\right)\int_0^\infty K_{vu}(\xi/\tau_{vu})d(\xi/\tau_{vu}) \approx 8.51\left(\frac{0.75+0.105\mathrm{Re}_p}{\mathrm{Re}_p}\right). \tag{32}$$

Note that $C_{vu} \to \infty$ when $\mathrm{Re}_p \to 0$, since in the zero Reynolds number limit the start of the faster t^{-2} decay is delayed to infinitely later time. Finite C_{vu} only exists for finite particle Reynolds number. Similar effective thermal history coefficient has been defined in the context of unsteady heat transfer by Balachandar and Ha (2001).

The Kolmogorov time scale is the shortest of all the eddy time scales and further we take the time scale of particle acceleration to be larger than the Kolmogorov time scale. If the particle is entrained in the turbulent flow for much longer time than τ_p, then its motion depends only on the turbulent eddies. Thus, if $\tau_{vu} \ll \tau_\eta$, then the viscous-unsteady force can be accurately approximated by the simpler expression given in Eq. (31). Otherwise, the traditional and more complex integral form of the viscous unsteady force, *i.e.*, Eq. (9), must be used. Thus the ratio

$$\frac{\tau_\eta}{\tau_{vu}} = \left(\frac{\eta}{d_p}\right)^2\left(\frac{\pi}{4}\right)^{1/3}\left(\frac{\mathrm{Re}_p}{0.75+0.105\mathrm{Re}_p}\right)^2. \tag{33}$$

plays an important role. In the above, Re_p is given by Eqs. (22) and (24), or (26) depending on the regime of relative particle time scale. Therefore, the ratio τ_η/τ_{vu} is a function of relative particle size (d_p/η), particle-to-fluid density ratio (ρ_p/ρ_f) and the intensity of turbulence given in terms of the length scale ratio (L/η). The dependence of τ_η/τ_{vu} on the three parameters is presented in Fig. 3. Clearly the results are insensitive to the precise value of L/η. It can be seen that in general $\tau_{vu} \geqslant \tau_\eta$, except for a narrow range of particle size around $d_p/\eta \sim 1$ when the particle-to-fluid density ratio is large. Even in this narrow range τ_{vu} is not too much smaller than τ_η.

We are thus led to the first major conclusion that the integral representation of the viscous unsteady force is unavoidable in the context of particle motion in a turbulent flow. This is a robust

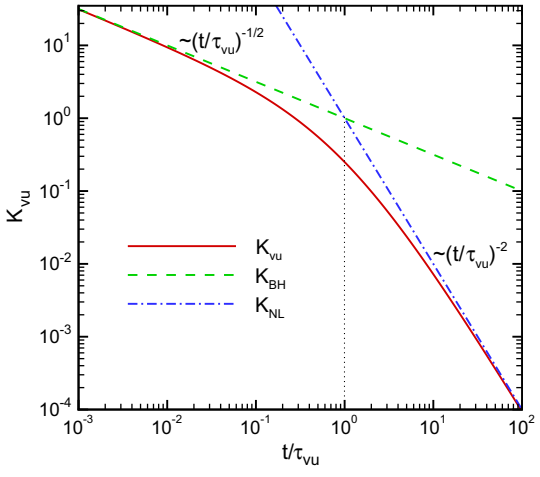

Fig. 2. Viscous-unsteady kernel K_{vu} as a function of t/τ_{vu}, compared to the Basset history kernel (K_{BH}) and the non-linear limit of the kernel (K_{NL}).

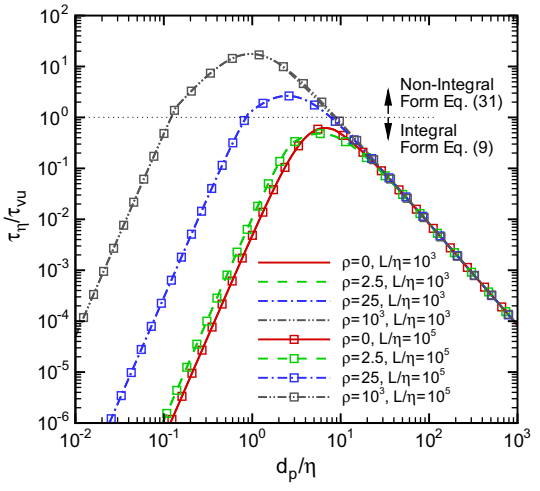

Fig. 3. The ratio between Kolmogorov and viscous-unsteady time scales (τ_η/τ_{vu}) as a function of d_p/η, ρ_p/ρ_f, and L/η.

conclusion and it applies for nearly all particle-to-fluid density ratios, size ratios and intensity of turbulence.

A related consequence is that for nearly all combinations of d_p/η, ρ_p/ρ_f, and L/η, there exists a range of small eddies of size η and larger whose acceleration makes the largest contribution to the viscous-unsteady force. Furthermore, the time scales of these eddies are smaller than τ_{vu}. As a result, the Basset-like slower $t^{-1/2}$ decay of the viscous unsteady kernel has the dominant contribution to the viscous unsteady force. Based on this argument, the viscous-unsteady force can be approximated in terms of fractional derivatives as

$$\mathbf{F}_{vu} \approx \frac{3}{2} d_p^2 \sqrt{\pi \nu} \left(\frac{D^{1/2} \rho_f \mathbf{u}_f}{Dt^{1/2}} - \frac{d^{1/2} \rho_f \mathbf{u}_p}{dt^{1/2}} \right). \tag{34}$$

This simplified form will henceforth be used to evaluate the importance of the viscous-unsteady force. This is the form used by Bagchi and Balachandar (2002) in their evaluation of the scaling of the viscous-unsteady force.

5. Importance of unsteady forces in forward coupling

The importance of the different unsteady force contributions to particle motion (forward momentum coupling) will be evaluated in terms of the ratio between the magnitudes of unsteady and quasi-steady forces. We recognize that the stress-gradient, added-mass, and viscous-unsteady forces arise from different mechanisms and therefore, we will discuss the importance of each of them separately.

In establishing their relative importance we will distinguish the three familiar approaches to resolve the fluid flow. In the context of direct numerical simulation (DNS), all the turbulent scales of the fluid phase are resolved and the importance of the unsteady forces in forward coupling will be evaluated with all the turbulent scales taken into account. In the other limit of Reynolds averaged Navier–Stokes (RANS) simulation of the fluid flow, only the mean flow motion is resolved. In the case of large eddy simulation (LES), only the dynamics of a range of large eddies are directly computed. In these later two cases the importance of the unsteady forces will be evaluated only in the context of the flow scales that are resolved and computed.

5.1. Importance of stress-gradient force

It can be easily shown that the ratio between $\mathbf{F}_{sg}$ and $\mathbf{F}_{qs}$ can be expressed as

$$\left| \frac{\mathbf{F}_{sg}}{\mathbf{F}_{qs}} \right| \approx \frac{I_{sg}}{\rho_p/\rho_f}, \tag{35}$$

where I_{sg} is defined as

$$I_{sg} = \frac{\tau_p' |D\mathbf{u}_f/Dt|}{|\mathbf{u}_f - \mathbf{u}_p|}. \tag{36}$$

From the above it is clear that the ratio between stress-gradient and quasi-steady forces on the particle depends on both the fluid-to-particle density ratio ρ_p/ρ_f and the correction function I_{sg}. Therefore, the conventional thought, that ρ_p/ρ_f is sufficient to evaluate the significance of unsteady forces, is valid only when $I_{sg} \sim O(1)$. A large value of the correction function could result in significant contribution from the stress-gradient force even in the case of large particle-to-fluid density ratio, if $I_{sg}/(\rho_p/\rho_f) \approx O(1)$. Thus, here we will seek an estimation of the correction function.

In the previous section we obtained an estimate of relative velocity and relative acceleration for a particle of time scale τ_p in the context of dispersed multiphase turbulence. With Eqs. (18) and (19), we can estimate I_{sg} as a function of ρ_p/ρ_f and St_l as

$$I_{sg} = \begin{cases} \frac{\mathrm{St}_l}{|1-\rho_f/\rho_p|}, & \text{if } \tau_l < \tau_{l^*}, \\ \frac{1}{|1-\rho_f/\rho_p|}, & \text{if } \tau_l > \tau_{l^*}. \end{cases} \tag{37}$$

The multiplicative factor, $|1-\rho_f/\rho_p|^{-1}$, approaches 1 for heavy particles ($\rho_p/\rho_f \gg 1$) and ρ_p/ρ_f for bubbles ($\rho_p/\rho_f \ll 1$). In the limit of neutrally buoyant particles ($\rho_p/\rho_f = 1$), $I_{sg} \to \infty$. Nevertheless, since the relative velocity for neutrally buoyant particles is generally zero (after a short transition time for the particle to catch up with the ambient flow), the stress-gradient force will then be the only active force in this limit, its importance over quasi-steady force is trivially established.

Regime I particles respond to all the flow times scales and the correction function depends only on the density ratio and is independent of the eddy size as

$$I_{sg} = \frac{1}{|1-\rho_f/\rho_p|}. \tag{38}$$

Regime III particles are too large to respond to any of the turbulent eddies and the correction function depends on the eddy size and takes the other limit of Eq. (37) for all the turbulent eddies as

$$I_{sg} = \frac{\mathrm{St}_l}{|1-\rho_f/\rho_p|}. \tag{39}$$

For particles that are in between in Regime II, the correction will follow Eq. (38) for the slower moving eddies of size larger than l^*, and will follow Eq. (39) for the faster eddies of size smaller than l^*.

The behavior of the correction function, scaled by $|1-\rho_f/\rho_p|$ is shown in Fig. 4(a). The largest value of the correction is always for the smallest turbulent eddy and can be expressed as

$$I_{sg,max} = \frac{\max(1, \mathrm{St}_\eta)}{|1-\rho_f/\rho_p|}, \tag{40}$$

where only for Regime I particles we have $I_{sg,\,max} = 1/|1-\rho_f/\rho_p|$. In other words, the relative importance of the stress-gradient force compared to the quasi-steady force is the strongest for the Kolmogorov scale eddies, provided the particle is in Regime II or III.

Let us choose a threshold value δ (say for Example 5% or $\delta = 0.05$), so that for values of the force ratios given in (25) larger than the threshold, we will consider the contribution of stress-gradient force to particle motion to be significant when compared to the quasi-steady force. With such a choice of threshold, in a direct numerical simulation (DNS) where the Kolmogorov eddies are fully resolved, the criterion for the importance of the stress-gradient force can be stated as

$$\textbf{DNS}: \qquad \frac{\rho_f}{\rho_p} \frac{\mathrm{St}_\eta}{|1-\rho_f/\rho_p|} > \delta. \tag{41}$$

(Note that since the point-particle approach is used in the present study, the term "DNS" here refers to point-particle DNS instead of particle-resolved DNS.) The above criterion is clearly satisfied for bubbles and near-neutral particles. This is fully consistent with current practice where unsteady forces such as stress-gradient and added-mass forces are included in the motion of bubbles and particles of density comparable to the fluid (i.e., for $\rho_p \lesssim O(\rho_f)$). Thus, the real use of the above criterion is in the case of much heavier-than-fluid particles. By taking the limit $\rho_p \gg \rho_f$ and making use of the relation $\tau_\eta = \eta^2/\nu$, we can simplify the above criterion as

$$\textbf{DNS}: \qquad \frac{d_p}{\eta} > \sqrt{18\delta}, \tag{42}$$

where η is the Kolmogorov length scale. To obtain the above criterion, Φ is taken to be unity due to the small Re_p (see Eq. (20)). It is

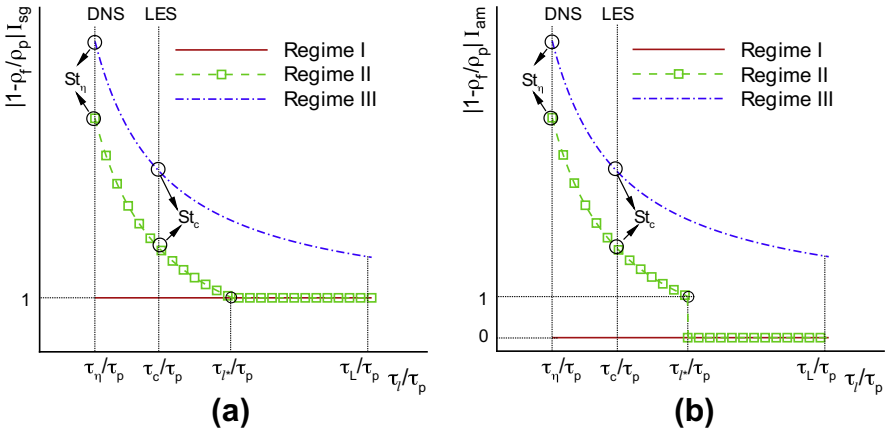

Fig. 4. Correction functions for the ratios of the (a) stress-gradient force (I_{sg}) and (b) added-mass force (I_{am}) compared to the quasi-steady force as functions of τ_l/τ_p for the three different regimes (Regime I: $\tau_p < \tau_\eta$; Regime II: $\tau_\eta < \tau_p < \tau_L$; Regime III: $\tau_p > \tau_L$).

now clear that, in the case of gas-particle multiphase flows the importance of the stress-gradient force depends on particle-to-fluid length scale ratio and not on the density ratio.

The above criterion has been derived based on the particle response to Kolmogorov scale eddies. If the above condition (Eq. (42)) is satisfied, it implies that the eddies of size equal to and slightly larger than Kolmogorov scale influence the particle motion not only through the quasi-steady force, but also through the stress-gradient force. This importance of the stress-gradient force may only be limited to the influence of the small scale turbulent eddies. Nevertheless, in the context of DNS, where all the scales of turbulent motion are fully and faithfully resolved, it is essential to similarly account for the influence of the entire range of flow scales on particle motion. Thus, the conditions given in Eqs. (41) and (42) are relevant for DNS and have been accordingly marked.

In the context of Reynolds averaged Navier–Stokes (RANS) simulations, only the largest scales of motion are resolved and computed. The only fluid time scale of relevance is the integral time scale τ_L. Thus, the criterion for the importance of the stress-gradient force in RANS multiphase flow simulations of heavier-than-fluid particles becomes

$$\textbf{RANS}: \quad \frac{\rho_f}{\rho_p}\mathrm{St}_L > \delta \quad \text{or} \quad \frac{d_p}{L} > \sqrt{18\delta}, \tag{43}$$

where L is the integral length scale. Based on the above condition it can be concluded that in gas-particle RANS simulations, the stress-gradient force can be ignored in the calculation of particle motion. It must be stressed that this assertion pertains only to the force computed based on the resolved Reynolds-averaged fluid motion. In RANS the fluid fluctuations at all the turbulent scales are not computed and thus their influence on particle motion must be modeled. Traditionally such modeling has been only based on the quasi-steady force due to the unresolved eddies. However, as we have seen above for DNS, if criterion (42) is satisfied, even in RANS simulations the closure relations for the fluctuating force on the particle must account for the stress-gradient force as well.

The above argument can be easily extended to large eddy simulations (LES), where a cut-off length scale l_c is defined, and only the dynamics of eddies larger than l_c are directly computed. In LES it is appropriate to rewrite the equation of particle motion (Eq. (5)) as

$$m_p\frac{d\mathbf{u}_p}{dt} = (\widetilde{\mathbf{F}}_{qs} + \widetilde{\mathbf{F}}_{sg} + \widetilde{\mathbf{F}}_{am} + \widetilde{\mathbf{F}}_{vu}) + (\widehat{\mathbf{F}}_{qs} + \widehat{\mathbf{F}}_{sg} + \widehat{\mathbf{F}}_{am} + \widehat{\mathbf{F}}_{vu}), \tag{44}$$

where the first four terms on the right are the quasi-steady and unsteady forces due to the resolved large eddy flow field, while the last four terms are the corresponding forces due to the unresolved scales of motion. The first four terms can be computed using deterministic expressions such as those given in Eqs. (6)–(9), with the fluid quantities given by the resolved large eddy flow field. In contrast, the last four terms need to be modeled as multiphase subgrid contribution, since the precise details of the unresolved scales are not available. The importance of the stress-gradient force arising from the resolved scales is evaluated in terms of the ratio, $|\widetilde{\mathbf{F}}_{sg}/\widetilde{\mathbf{F}}_{qs}|$. This gives rise to the criterion

$$\textbf{LES}: \quad \frac{\rho_f}{\rho_p}\mathrm{St}_c > \delta \quad \text{or} \quad \frac{d_p}{l_c} > \sqrt{18\delta}, \tag{45}$$

where $\mathrm{St}_c = \tau_p/\tau_c$ and τ_c is the time scale of the smallest resolved eddies of size l_c. If the above criterion is satisfied, then the stress-gradient force due to the smallest resolved scales is important and the deterministic stress-gradient force $\widetilde{\mathbf{F}}_{sg}$ must be included in the LES equation of particle motion. When the above criterion is not satisfied, the deterministic portion of particle motion can be computed based only on $\widetilde{\mathbf{F}}_{qs}$. Even then, as argued for RANS, if Eq. (42) is satisfied, the contribution from $\widehat{\mathbf{F}}_{sg}$ due the unresolved small scales becomes comparable to $\widehat{\mathbf{F}}_{qs}$ and must be accounted in multiphase subgrid modeling.

5.2. Importance of added-mass force

Similar to the stress-gradient force, the relative importance of the added-mass force can be evaluated by the ratio between the added-mass and quasi-steady forces, which can be written as

$$\left|\frac{\mathbf{F}_{am}}{\mathbf{F}_{qs}}\right| \approx \frac{C_M I_{am}}{\rho_p/\rho_f}, \tag{46}$$

where I_{am} is defined as

$$I_{am} = \frac{\tau_p'\left|\frac{D\mathbf{u}_f}{Dt} - \frac{d\mathbf{u}_p}{dt}\right|}{|\mathbf{u}_f - \mathbf{u}_p|}. \tag{47}$$

By Eqs. (18) and (19), we can estimate I_{am} for the l-size eddy as

$$I_{am} = \begin{cases} 0, & \text{if } \mathrm{St}_l < 1, \\ I_{sg}, & \text{if } \mathrm{St}_l > 1. \end{cases} \tag{48}$$

As a result, $I_{am} = 0$ for Regime I particles. For Regime III particles I_{am} is identical to I_{sg}. In Regime II, $I_{am} = 0$ when $\tau_l > \tau_{l*}$ and $I_{am} = I_{sg}$ when $\tau_l < \tau_{l*}$. A schematic of I_{am} is plotted in Fig. 4(b). It can be seen that the relative importance of the added-mass force is again strongest for the Kolmogorov scale eddies. The maximum values of I_{am} in Re-

gimes II and III are identical to those for I_{sg}. Therefore, the criterion for the importance of the added-mass force is quite similar to the stress-gradient force, which is expressed as

$$\textbf{DNS}: \quad \frac{\rho_f}{\rho_p}\mathrm{St}_\eta > \frac{\delta}{C_M} \quad \text{or} \quad \frac{d_p}{\eta} > \sqrt{\frac{18\delta}{C_M}}. \tag{49}$$

Since the added-mass coefficient C_M is an $O(1)$ quantity, the analysis above for the importance of the stress-gradient force in DNS, RANS, and LES discussed in Section 5.1 is applicable to the added-mass force.

5.3. Importance of viscous-unsteady force

The ratio between the viscous-unsteady and quasi-steady forces is expressed as

$$\left|\frac{\mathbf{F}_{vu}}{\mathbf{F}_{qs}}\right| \approx \zeta \frac{I_{vu}}{\sqrt{\rho_p/\rho_f}}, \tag{50}$$

where I_{vu} is defined as

$$I_{vu} = \frac{\sqrt{\tau_p'}\left|\frac{D^{1/2}\mathbf{u}_f}{Dt^{1/2}} - \frac{d^{1/2}\mathbf{u}_p}{dt^{1/2}}\right|}{|\mathbf{u}_f - \mathbf{u}_p|}. \tag{51}$$

The coefficient ζ is defined as

$$\zeta = \frac{3}{\sqrt{2\pi\Phi(\mathrm{Re}_p)}}. \tag{52}$$

Similar to relative acceleration, the term $|D^{1/2}\mathbf{u}_f/Dt^{1/2} - d^{1/2}\mathbf{u}_p/dt^{1/2}|$ can be estimated as

$$\left|\frac{D^{1/2}\mathbf{u}_f}{Dt^{1/2}} - \frac{d^{1/2}\mathbf{u}_p}{dt^{1/2}}\right| \approx \begin{cases} 0, & \text{if } \mathrm{St}_l < 1, \\ \frac{u_l}{\sqrt{\tau_l}}, & \text{if } \mathrm{St}_l > 1. \end{cases} \tag{53}$$

Then it can be easily shown that

$$I_{vu} = I_{am}\sqrt{\frac{\tau_l}{\tau_p'}}, \tag{54}$$

Similar to I_{am} and I_{sg}, the maximum value of I_{vu} is dictated by the Kolmogorov eddies.

For bubbles and near-neutrally buoyant particles, it is clear that the viscous-unsteady force is comparable to the quasi-steady force. Therefore, the further discussion will focus on the heavy particles ($\rho_p \gg \rho_f$). In the limit of $\rho_p \gg \rho_f$, the ratio between viscous-unsteady and quasi-steady forces can be related to that between added-mass and quasi-steady forces as

$$\left|\frac{\mathbf{F}_{vu}}{\mathbf{F}_{qs}}\right| \sim \sqrt{\left|\frac{\mathbf{F}_{am}}{\mathbf{F}_{qs}}\right|}. \tag{55}$$

It is now clear that when added-mass force is important in evaluating the motion of a particle (i.e., $|\mathbf{F}_{am}/\mathbf{F}_{qs}| \geqslant O(1)$), the corresponding viscous-unsteady force will also be of importance. If added-mass force can be ignored then viscous unsteady force can also be ignored. Thus the criterion for DNS, RANS, and LES given in Eqs. (42), (43) and (45) applies for viscous unsteady force as well.

The increasing importance of the unsteady forces, and as a consequence inability of the quasi-steady force alone to accurately model the actual time history of forces on a particle of size larger than the Kolmogorov scale has been observed in particle-resolved DNS of isotropic and wall-bounded turbulent flows over a particle, see Bagchi and Balachandar (2003), Merle et al. (2005) and Zeng et al. (2008). Point-particle approach is theoretically well grounded only in the limit when the particle size is much smaller than the grid resolution, which in turn is of the order of the smallest resolved fluid scale. There have been recent advancements to extend the point-particle approach to finite-sized particles which are comparable to the grid size. Nevertheless, the above scaling analysis shows that the unsteady forces will be of importance provided particle size is comparable or larger than the Kolmogorov scale. It must however be cautioned that the present scaling analysis only establishes the importance of the unsteady forces in the case of particles of size larger than the Kolmogorov scale, but does not provide a closure model for the unsteady forces that can be reliably used in the point particle approach. The difficulty arises from the fact that the particle Reynolds number for such finite-sized particles is generally large that non-linear effects become strong. Furthermore, self-induced vortex shedding in the particle wake begins to strongly influence the momentum and thermal coupling. The resulting force and heat transfer fluctuations are not fully correlated with the fluctuations of the oncoming flow approaching the particle, and thus their modeling can at best be only stochastic. Nevertheless, the above scaling analysis shows that such complications begin to arise for particles of $d_p > \eta$ through the importance of the unsteady forces.

5.4. Unsteady forces when shock-particles interactions are involved

Compressible multiphase flows that involve shock-particle interaction present an interesting example. While the fluid properties can jump across the shock discontinuity, the particle properties have to adjust gradually through a transient process due to finite particle inertia, see Rudinger (1964). As a result, during a short duration following shock-particle interaction, the fluid and particles are far away from "equilibrium," and thus the equilibrium Eulerian approximation in Eq. (16) cannot be used for shock-particle interaction.

As the particle properties vary little during and soon after the shock passage, it is taken that $d\mathbf{u}_p/dt = 0$, *i.e.*, the "frozen" approximation, see Ling et al. (2009). Then the relative velocity can be approximated by

$$|\mathbf{u}_f - \mathbf{u}_p| \approx \Delta u_f, \tag{56}$$

where Δu_f represents the fluid velocity jump across the shock. Similarly, the relative acceleration is equal to the gas acceleration, which is estimated as

$$\left|\frac{D\mathbf{u}_f}{Dt} - \frac{d\mathbf{u}_p}{dt}\right| = \left|\frac{D\mathbf{u}_f}{Dt}\right| \approx \frac{\Delta u_f}{\tau_s} \tag{57}$$

where τ_s is the time it takes for the shock to pass over the particle. When shock thickness is smaller than the particle size, d_p is the appropriate length scale and the shock-passage time scale, τ_s, can be approximated as

$$\tau_s \approx \frac{d_p}{u_s}, \tag{58}$$

where u_s denotes the shock propagation speed, see Ling et al. (2013).

As a result, the ratios of the stress-gradient and added-mass forces to the quasi-steady force can be approximated as

$$\left|\frac{\mathbf{F}_{sg}}{\mathbf{F}_{qs}}\right| \approx \left|\frac{\mathbf{F}_{am}}{\mathbf{F}_{qs}}\right| \approx \frac{\rho_f}{\rho_p}\frac{\tau_p'}{\tau_s} = \frac{u_s d_p}{18\nu} \sim \frac{d_p}{\lambda}\frac{\mathrm{M}_s}{\mathrm{M}_s - 1}, \tag{59}$$

where λ denotes the shock thickness, which scales as

$$\lambda \sim \frac{\nu}{c_{f,0}(\mathrm{M}_s - 1)}. \tag{60}$$

The shock Mach number M_s is defined as

$$\mathrm{M}_s = \frac{u_s}{c_{f,0}}, \tag{61}$$

where, $c_{f,0}$ is the ambient fluid speed of sound before the shock arrival. As can be seen in Eq. (59), when $d_p > \lambda$, the ratio between unsteady to quasi-steady forces will be larger than one, namely that unsteady forces are important in momentum coupling. This result is completely consistent with the analysis of turbulent flow in Sections 5.1,5.2,5.3. Here the shock thickness λ plays the role of the Kolmogorov scale. As a result, provided $d_p/\lambda \gtrsim 1$, unsteady forces are of importance.

It can be shown that, for heavy particles ($\rho_p \gg \rho_f$), $|\mathbf{F}_{vu}/\mathbf{F}_{qs}|$ scales as $\sqrt{|\mathbf{F}_{am}/\mathbf{F}_{qs}|}$, therefore, when $d_p > \lambda$, the viscous-unsteady force will also be important compared to the quasi-steady force. Furthermore, Eq. (55) can be rewritten as

$$\left|\frac{\mathbf{F}_{am}}{\mathbf{F}_{vu}}\right| \sim \left|\frac{\mathbf{F}_{vu}}{\mathbf{F}_{qs}}\right| \sim \sqrt{\left|\frac{\mathbf{F}_{am}}{\mathbf{F}_{qs}}\right|}, \tag{62}$$

from which it is clear that in problems such as shock-particle interaction where $|\mathbf{F}_{am}/\mathbf{F}_{qs}| \gg 1$, the viscous-unsteady force will be small compared to the added-mass force. In such cases, both quasi-steady and viscous-unsteady forces can be ignored, and only the inviscid forces (the stress-gradient and added-mass forces) need to be accounted in momentum coupling. This is consistent with the observations in previous works that inviscid mechanisms dominate in the early stage of shock-particle interaction, see Zhang et al. (2003), Parmar et al. (2009), Ling et al. (2011a) and Ling et al. (2013).

It should be noted that the above simple estimate of the ratio between unsteady and quasi-steady forces ignores some of the details in shock-particle interaction, such as fluid density variation, shock reflection and refraction, and the compressibility effect on quasi-steady force, see Parmar et al. (2010). Therefore, Eq. (59) is only an estimate. Systematic analysis of unsteady forces in shock-particle interaction for a wide range of parameters can be found in previous works by Parmar et al. (2009) and Ling et al. (2011a,b). At last, it should also be reminded that, the dominance of the inviscid forces is limited to a short period of time during, and immediately after, the shock-particle interaction. The long term motion of the particle will be dictated by the quasi-steady force, as discussed by Parmar et al. (2009); Ling et al. (2011a).

6. Importance of quasi-steady and unsteady forces in backward momentum coupling

The backward coupling of particles on the fluid motion appears as the term $\sum_i \mathbf{F}_{fp,i}/\mathbb{V}$ in the momentum Eq. (2). If we consider a small control volume and carry out a volume-average of the forces exerted on all the particles inside the volume, then we have

$$\frac{1}{\mathbb{V}}\sum_i (\mathbf{F}_{qs,i} + \mathbf{F}_{sg,i} + \mathbf{F}_{am,i} + \mathbf{F}_{vu,i}) \approx \rho_p \phi_p (\mathbf{f}_{qs} + \mathbf{f}_{sg} + \mathbf{f}_{am} + \mathbf{f}_{vu}), \tag{63}$$

where ϕ_p is the volume-averaged particle volume fraction and $\mathbf{f}_{qs}$,-$\mathbf{f}_{sg}$,$\mathbf{f}_{am}$, and $\mathbf{f}_{vu}$ are the quasi-steady, stress-gradient, added-mass, and viscous-unsteady forces per unit mass averaged over the control volume. Then the fluid momentum equation, Eq. (2), can be written as

$$\rho_f \phi_f \frac{D\mathbf{u}_f}{Dt} - \nabla \cdot \boldsymbol{\sigma}_f = -\rho_p \phi_p (\mathbf{f}_{qs} + \mathbf{f}_{sg} + \mathbf{f}_{am} + \mathbf{f}_{vu}). \tag{64}$$

6.1. Quasi-steady force

To assess the importance of different force contributions in backward momentum coupling, we investigate the momentum coupling parameter corresponding to each force contribution separately. The momentum coupling parameter is defined as the ratio between the backward coupling force contribution and the inertial term in the fluid momentum equation. For example, the momentum coupling parameter of the quasi-steady force, Π_{qs}, is defined as

$$\Pi_{qs} = \frac{|\rho_p \phi_p \mathbf{f}_{qs}|}{|\rho_f \phi_f \frac{D\mathbf{u}_f}{Dt}|}. \tag{65}$$

When the momentum coupling parameter is large, the back effect of the force contribution on momentum coupling is significant.

By Eqs. (6) and (36), Π_{qs} can be expressed as

$$\Pi_{qs} \approx \frac{Y_p}{Y_f}\frac{1}{I_{sg}}, \tag{66}$$

where Y_p and Y_f are the mass fractions of particles and fluid. As can be expected, the importance of the quasi-steady force in backward momentum coupling with the fluid dominantly depends on the mass fraction ratio. In other words, when particle mass fraction is comparable to the fluid mass fraction, the back effect of quasi-steady force will influence the fluid motion. However, similar to Eq. (35), a correction function appears as $1/I_{sg}$. The quasi-steady force can be ignored in backward momentum coupling, only if $Y_p/(Y_f I_{sg})$ is negligibly small for every eddy size in the flow.

Similar to the analysis of Section 5.1, to evaluate the importance of the quasi-steady force in backward momentum coupling, we only need to focus on the maximum value of $1/I_{sg}$, which is attained for the largest integral scale eddies. For Regime I and II particles, $\max(1/I_{sg}) = |1 - \rho_f/\rho_p|$; while for Regime III particles, $\max(1/I_{sg}) = |1 - \rho_f/\rho_p|/\mathrm{St}_L$.

Therefore, the maximum values of coupling parameter of the quasi-steady force in different regimes can be approximated as

$$\Pi_{qs} \approx \begin{cases} \left|1 - \frac{\rho_f}{\rho_p}\right| \frac{Y_p}{Y_f}, & \text{Regimes I \& II } (\mathrm{St}_L < 1), \\ \left|1 - \frac{\rho_f}{\rho_p}\right| \frac{Y_p}{Y_f}\frac{1}{\mathrm{St}_L}, & \text{Regimes III } (\mathrm{St}_L > 1). \end{cases} \tag{67}$$

For heavy particles, the above expression reduces to

$$\Pi_{qs} \approx \begin{cases} \frac{Y_p}{Y_f}, & \text{Regimes I \& II}, \\ \frac{Y_p}{Y_f}\frac{1}{\mathrm{St}_L}, & \text{Regimes III}. \end{cases} \tag{68}$$

Conventionally, the momentum coupling parameter of the quasi-steady force is taken to be the mass fraction ratio Y_p/Y_f. As shown above, this is true only for Regime I and II particles whose $\mathrm{St}_L < 1$. For Regime III particles (i.e., for $\mathrm{St}_L > 1$), Π_{qs} depends on the product of Y_p/Y_f and $1/\mathrm{St}_L$. Similar relationship between the momentum coupling parameter and Stokes number was reported by Crowe et al. (1998). This result may seem puzzling. To help better understand the physical meaning of Π_{qs} for large St_L, we can rewrite Eq. (68) for Regime III particles as

$$\Pi_{qs} \approx 18\frac{\phi_p}{\phi_f}\left(\frac{\eta}{d_p}\right)^2 \mathrm{Re}_L^{1/2}\Phi(\mathrm{Re}_p), \tag{69}$$

where Re_L is the Reynolds number based on the integral scale eddies, which is in general much greater than 1. It can be observed that Π_{qs} in Eq. (69) will be small only in the case of particle size much larger than the Kolmogorov scale, *i.e.*, $\eta/d_p \ll O(1)$. It is know from Section 5.1 that under such condition, the unsteady forces become more important in momentum coupling. As a consequence, even though the contribution of the quasi-steady force in backward momentum coupling is small, fluid and particles are still two-way coupled since the backward momentum coupling is mainly due to the unsteady forces.

For bubbles, the momentum coupling parameter of the quasi-steady force given in Eq. (67) can be simplified as

$$\Pi_{qs} \approx \begin{cases} \frac{\phi_p}{\phi_f}, & \text{Regimes I \& II,} \\ \frac{\phi_p}{\phi_f}\frac{1}{\mathrm{St}_L}, & \text{Regimes III.} \end{cases} \tag{70}$$

Compared to the case of heavy particles, Π_{qs} in the limit of bubbles ($\rho_f/\rho_p \gg 1$) depends on particle volume fraction, instead of mass fraction. In Regime III, unsteady forces are dominant in backward momentum coupling. It can be observed that Eqs. (68) and (70), which account for the effect of particle time scales and density ratio, give more accurate evaluation on the momentum coupling parameter of the quasi-steady force than the conventional criterion based only on mass fraction ratio.

6.2. Stress-gradient force

The momentum coupling parameter of the stress-gradient force can be expressed as

$$\Pi_{sg} = \frac{|\rho_p \phi_p \mathbf{f}_{sg}|}{|\rho_f \phi_f \frac{D\mathbf{u}_f}{Dt}|} = \frac{\phi_p}{\phi_f}. \tag{71}$$

Therefore, the importance of the backward contribution of stress-gradient force depends only on particle volume fraction.

6.3. Added-mass force

The momentum coupling parameter of the added-mass force can be expressed as

$$\Pi_{am} = \frac{|\rho_p \phi_p \mathbf{f}_{am}|}{|\rho_f \phi_f \frac{D\mathbf{u}_f}{Dt}|} \approx \begin{cases} 0, & \text{Regimes I,} \\ C_M \frac{\phi_p}{\phi_f}, & \text{Regimes II \& III.} \end{cases} \tag{72}$$

Therefore, for Regime II and III particles (i.e., for $\mathrm{St}_\eta > 1$), the importance of the added-mass force to backward momentum coupling depends again on the particle volume fraction.

6.4. Viscous-unsteady force

The momentum coupling parameter of the viscous-unsteady force can be expressed as

$$\Pi_{vu} = \frac{|\rho_p \phi_p \mathbf{f}_{vu}|}{|\rho_f \phi_f \frac{D\mathbf{u}_f}{Dt}|} \approx \begin{cases} 0, & \mathrm{St}_l < 1, \\ \sqrt{\frac{\phi_p}{\phi_f}}\sqrt{\left(1+\frac{\rho_f}{2\rho_p}\right)\frac{Y_p}{Y_f}\frac{\tau_l}{\tau_p}}, & \mathrm{St}_l > 1. \end{cases} \tag{73}$$

The maximum value of Π_{vu} in the different regimes can be approximated as

$$\Pi_{vu} \approx \begin{cases} 0, & \text{Regime I,} \\ \sqrt{\frac{\phi_p}{\phi_f}}\sqrt{\left(1+\frac{\rho_f}{2\rho_p}\right)\frac{Y_p}{Y_f}}, & \text{Regime II,} \\ \sqrt{\frac{\phi_p}{\phi_f}}\sqrt{\left(1+\frac{\rho_f}{2\rho_p}\right)\frac{Y_p}{Y_f}\frac{1}{\mathrm{St}_L}}, & \text{Regime III.} \end{cases} \tag{74}$$

With Eqs. (68) and (70), the above estimate of Π_{vu} can be rewritten in terms of Π_{qs} and Π_{am} for both heavy particles and bubbles as

$$\Pi_{vu} \approx \sqrt{\Pi_{qs}\Pi_{am}}. \tag{75}$$

Eq. (75) is consistent with Eq. (55). It is interesting to notice that, in the case of heavy particles ($\rho_p \gg \rho_f$), while the Π_{qs} and Π_{am} depend on Y_p and ϕ_p, respectively, the momentum coupling parameter of the viscous-unsteady depends on both Y_p and ϕ_p, since it is related to both viscous and unsteady mechanisms.

7. Conclusions

Modeling of interphase coupling is critical to accurate simulation of dispersed multiphase flows. In this paper, we address three important fundamental questions about interphase coupling: (1) *Is it possible to simplify the integral representation of viscous-unsteady force?* (2) *Under what conditions unsteady forces are important in forward momentum coupling?* (3) *What parameters accurately evaluate the back effect of both the quasi-steady and unsteady forces in the fluid momentum equation?* The key findings of the present study in regard to these three questions are summarized separately as follows.

7.1. Conclusions on the representation of the viscous-unsteady force

In general, the viscous-unsteady force is given by a Basset-like convolution integral, whose computation is often costly. However, when both the particle and the surrounding fluid acceleration are sufficiently slow, it is possible to simplify the viscous-unsteady force and avoid evaluating the convolution integral. Here we establish the conditions under which such a simplification can be made. The main conclusions are:

- Only when the viscous-unsteady time scale τ_{vu} (defined as the transition time for the kernel to change from the slower $t^{-1/2}$ decay to the faster t^{-2} decay) is smaller than all the fluid time scales, the viscous-unsteady force formulation can be simplified. The resulting simplified viscous unsteady force given in Eq. (31) has a form similar to the added-mass force.
- In turbulent multiphase flows, τ_{vu} is larger than the Kolmogorov time scale τ_η under most circumstances. Therefore, the viscous-unsteady force generally needs to be calculated using the convolution history integral.
- For large particle-to-fluid density ratio ($\rho_p \gg \rho_f$), there exist a narrow range of particle size (d_p) around the Kolmogorov length scale (η) (see Fig. 3), for which $\tau_{vu} < \tau_\eta$ and the simplified form of viscous-unsteady force (Eq. (31)) can be used.

7.2. Conclusions on the importance of unsteady forces in forward momentum coupling

The ratio between the magnitudes of unsteady and quasi-steady forces is used to evaluate the importance of the unsteady forces in forward momentum coupling. Key conclusions in regard to the importance of the unsteady forces in forward momentum coupling include:

- Unsteady forces are important in evaluating the motion of particles of density comparable or smaller than that of the surrounding fluid (*i.e.*, when $\rho_p \lesssim O(\rho_f)$).
- Conventionally, the unsteady forces are neglected in gas-particle flows. The present scaling analysis shows that for particles much heavier than the fluid (*i.e.*, $\rho_p \gg \rho_f$) the importance of the unsteady forces depends on the ratio between the particle size and the smallest fluid length scale and not on the particle-to-fluid density ratio.
- In DNS of turbulent multiphase flows, the intent is to accurately compute all the turbulent length scales and their influence on particle motion. When the particle size is comparable or larger than the Kolmogorov scale (*i.e.*, smallest fluid length scale), unsteady forces due to the smallest eddies are important in accurately evaluating the particle

motion. In LES and RANS, when the particle size is larger than the smallest resolved scale, the unsteady forces due to the resolved fluid flow will be important and must be included in the computation of the deterministic component of particle motion. When the particle size is smaller than the resolved scale but larger than the Kolmogorov scale, unsteady forces due to the unresolved scales remain important and must be accounted in the closure models. Again, we should remind that for the case of particles of size larger than the Kolmogorov scale, the present scaling analysis only establishes the importance of the unsteady forces, but does not provide a closure model for the unsteady forces that can be reliably used in the point particle approach.

- In shock-particle interaction, since the particle size is generally larger than the shock thickness (i.e., the smallest flow length scale), the unsteady forces dominate the quasi-steady force during shock-particle interaction.
- For heavy particles (*i.e.*, $\rho_p \gg \rho_f$), we observe the stress gradient and added-mass forces to be of the same order and the ratio between viscous-unsteady and quasi-steady forces to scale as the square root of the ratio between the added-mass and quasi-steady forces, *i.e.*, $|\mathbf{F}_{vu}/\mathbf{F}_{qs}| \sim \sqrt{|\mathbf{F}_{am}/\mathbf{F}_{qs}|}$. Therefore, in situations where the inviscid forces ($\mathbf{F}_{sg}$ and $\mathbf{F}_{am}$) dominate the quasi-steady force, they also dominate the viscous unsteady force.

7.3. Conclusions on the importance of quasi-steady and unsteady forces in backward momentum coupling

We define momentum coupling parameters as the ratio between the back contribution to the fluid momentum equation from the coupling force and the fluid inertial term. The momentum coupling parameter of each force contribution is estimated through scaling argument. The key conclusions are:

- The mass fraction ratio, Y_p/Y_f, is usually taken to evaluate the importance of the quasi-steady force in backward momentum coupling. It is shown by the scaling analysis that the momentum coupling parameter of the quasi-steady force Π_{qs} depends on the particle mass and volume fraction ratios for heavy particles and bubbles, respectively. For heavy particles with time scale larger than the turbulence integral time scale ($\tau_p > \tau_L$), $\Pi_{qs} \approx Y_p/(Y_f \mathrm{St}_L)$ (Eq. (68)). When $\mathrm{St}_L \gg 1$, the back effect of quasi-steady force on the fluid motion is small and unsteady forces become dominant in backward momentum coupling.
- The momentum coupling parameters of stress-gradient and added-mass forces are similar. The contributions of the stress-gradient and added-mass forces to backward coupling is related to the particle volume fraction.
- The momentum coupling parameter of the viscous-unsteady force scales as the square root of the products of the momentum coupling parameters of quasi-steady and added-mass forces. Therefore, for heavy particles, the back effect of the viscous-unsteady force on fluid motion depends on both particle mass and volume fractions.

At last, it should be reminded that significant simplifications and approximations have been made to achieve the present scaling results. The multiphase flows are considered to be dilute and the effect of gravity is ignored. It has also been assumed that, the particles have been entrained into the fluid flow for a long enough time so that the initial conditions of the particles are forgotten. Nevertheless, we believe the present results provide useful guideline for future development of accurate simulation approaches for dispersed multiphase flows. Following the scaling analysis in the present paper, one can systematically incorporate the effects of finite particle volume fraction, gravity, and particle initial conditions to obtain scaling results for the problems in which these effects are important.

Acknowledgment

The authors would like to acknowledge support from AFOSR (FA9550-10-1-0309).

Appendix A. Calculation of added-mass (inviscid-unsteady) force

In compressible flows, the added-mass force needs to be expressed as a history integral similar to the viscous-unsteady force due to the finite speed of sound, see Longhorn (1952) and Parmar et al. (2008). The added-mass force in compressible flows is referred as inviscid-unsteady force by Parmar et al. (2008) and is given as

$$\mathbf{F}_{am} = V_p \int_{-\infty}^{t} K_{iu}\left(\frac{t-\xi}{\tau_{iu}}, \mathrm{M}_p\right)\left(\frac{D\rho_f \mathbf{u}_f}{Dt} - \frac{d\rho_f \mathbf{u}_p}{dt}\right)\frac{d\xi}{\tau_{iu}}, \tag{A.1}$$

where the inviscid-unsteady time scale τ_{iu} is defined as

$$\tau_{iu} = \frac{d_p}{c_{f,0}}. \tag{A.2}$$

where $c_{f,0}$ is the ambient fluid speed of sound. Definition of the particle Mach number M_p is given in Eq. (12). The inviscid-unsteady kernel function is denoted by K_{iu}. In the limit of zero particle Mach number, K_{iu} for an isolated spherical particle is given by Longhorn (1952) as

$$K_{iu}(t/\tau_{iu}) = \exp(-2t/\tau_{iu})\cos(2t/\tau_{iu}). \tag{A.3}$$

It can be observed that K_{iu} decays exponentially on the inviscid-unsteady time scale. The inviscid-unsteady kernel for finite M_p was computed numerically by Parmar et al. (2008) and it was shown that τ_{iu} varies little with M_p.

If the time scale of relative acceleration is much larger than τ_{iu}, then the term $D\rho_f\mathbf{u}_f/Dt - d\rho_f\mathbf{u}_p/dt$ in Eq. (A.1) can be taken outside of the integral. The integral of K_{iu} can be precomputed, yielding an effective added-mass coefficient $C_M = \int_0^\infty K_{iu}(\xi)d\xi$. Then Eq. (A.1) reduces to Eq. (8).

In a turbulent multiphase flow, the smallest fluid time scale is the Kolmogorov scale τ_η. Therefore, the time scale ratio τ_η/τ_{iu} determines whether the simpler form (Eq. (8)) can be used to calculate the inviscid-unsteady force instead of the integral form (Eq. (A.1)). The expression of τ_η/τ_{iu} is given as

$$\frac{\tau_\eta}{\tau_{iu}} = \frac{\eta}{d_p}\frac{1}{\mathrm{M}_\eta}, \tag{A.4}$$

where the Mach number based on the Kolmogorov velocity scale is defined as $\mathrm{M}_\eta = u_\eta/c_{f,0}$. The fluid speed of sound is typically three or more orders of magnitude larger than the Kolmogorov velocity scale. Thus, for practical range of d_p, $\tau_\eta/\tau_{iu} \gg 1$, and therefore, the simpler Eq. (8) is sufficient to compute the inviscid-unsteady force in a turbulent multiphase flow.

Nevertheless, it should be reminded that, if there exists a fluid time scale that is smaller than the Kolmogorov time scale, then the above conclusion must be reconsidered. For example, in case of shock-particle interaction, the shock-passage time scale τ_s (defined in Eq. (58)) is typically quite small. Then τ_s/τ_{iu} instead of τ_η/τ_{iu} should be used in evaluating the convolution integral (Eq. (A.1)). The expression for τ_s/τ_{iu} is given as

$$\frac{\tau_s}{\tau_{iu}} = \frac{1}{M_s}. \tag{A.5}$$

According to the definition of the shock Mach number in Eq. (61), $M_s \geqslant 1$ and thus $\tau_s/\tau_{iu} \leqslant 1$. Therefore, the integral form Eq. (A.1) is needed in flows that involve shock-particle interactions, see Parmar et al. (2009).

References

Balachandar, S., Eaton, J.K., 2010. Turbulent dispersed multiphase flow. Annu. Rev. Fluid Mech. 42, 111–133.

Ling, Y., Haselbacher, A., Balachandar, S., Najjar, F.M., Stewart, D.S., 2013. Shock interaction with a deformable particle: direct numerical simulations and point-particle modeling. J. Appl. Phys. 113, 013504.

Maxey, M.R., Riley, J.J., 1983. Equation of motion for a small rigid sphere in a nonuniform flow. Phys. Fluids 26, 883–889.

Gatignol, R., 1983. The Faxén formulae for a rigid particle in an unsteady non-uniform Stokes flow. J. Mech. Theor. Appl. 1, 143–160.

Parmar, M., Haselbacher, A., Balachandar, S., 2011. Generalized Basset–Boussinesq–Oseen equation for unsteady forces on a sphere in a compressible flow. Phys. Rev. Lett. 106, 084501.

Parmar, M., Haselbacher, A., Balachandar, S., 2012. Equation of motion for a sphere in equation of motion for a sphere in non-uniform compressible flows. J. Fluid Mech. 699, 352–375.

Bagchi, P., Balachandar, S., 2002. Steady planar straining flow past a rigid sphere at moderate Reynolds number. J. Fluid Mech. 466, 365–407.

Pougatch, K., Salcudean, M., Chan, E., Knapper, B., 2008. Modelling of compressible gas–liquid flow in a convergent–divergent nozzle. Chem. Eng. Sci. 63 (16), 4176–4188.

Snider, D.M., O'Rourke, P.J., Andrews, M.J., 1998. Sediment flow in inclined vessels calculated using a multiphase particle-in-cell model for dense particle flows. Int. J. Multiphase Flow 24, 1359–1382.

Patankar, N.A., Joseph, D.D., 2001. Modeling and numerical simulation of particulate flows by the Eulerian–Lagrangian approach. Int. J. Multiphase Flow 27 (10), 1659–1684.

Parmar, M., Haselbacher, A., Balachandar, S., 2009. Modeling of the unsteady force for shock–particle interaction. Shock Waves 19, 317–329.

Ling, Y., Haselbacher, A., Balachandar, S., 2011a. Importance of unsteady contributions to force and heating for particles in compressible flows. Part 1: Modeling and analysis for shock–particle interaction. Int. J. Multiphase Flow 37, 1026–1044.

Ling, Y., Haselbacher, A., Balachandar, S., 2011b. Importance of unsteady contributions to force and heating for particles in compressible flows. Part 2: Application to particle dispersal by blast wave. Int. J. Multiphase Flow 37, 1013–1025.

Crowe, C.T., Sommerfield, M., Tsuji, Y., 1998. Multiphase Flows with Droplets and Particles. CRC Press.

Subramaniam, S., 2013. Lagrangian–Eulerian methods for multiphase flows. Prog. Energ. Combust. Sci. 39, 215–245.

Garg, R., Narayanan, C., Lakehal, D., Subramaniam, S., 2007. Accurate numerical estimation of interphase momentum transfer in Lagrangian–Eulerian simulations of dispersed two-phase flows. Int. J. Multiphase Flow 33, 1337–1364.

Ling, Y., Haselbacher, A., Balachandar, S., 2010. A numerical source of small-scale number-density fluctuations in Eulerian–Lagrangian simulations of multiphase flows. J. Comput. Phys. 229, 1828–1851.

Balachandar, S., 2009. A scaling analysis for point particle approaches to turbulent multiphase flows. Int. J. Multiphase Flow 35, 801–810.

Squires, K.D., Eaton, J.K., 1991. Preferential concentration of particles by turbulence. Phys. Fluids A 3 (5), 1169–1178.

Elghobashi, S., Truesdell, G.C., 1992. Direction simulation of particle dispersion in a decaying isotropic turbulence. J. Fluid Mech. 242, 655–700.

Andrews, M.J., O'Rourke, P.J., 1996. The multiphase particle-in-cell (MP-PIC) method for dense particulate flows. Int. J. Multiphase Flow 22 (2), 379–402.

Balakrishnan, K., Nance, D., Menon, S., 2010. Simulation of impulse effects from explosive charges containing metal particles. Shock Waves 20, 217–239.

Ling, Y., Wagner, J.L., Beresh, S.J., Kearney, S.P., Balachandar, S., 2012. Interaction of a planar shock wave with a dense particle curta: modeling and experiments. Phys. Fluids 24, 113301.

Crowe, C.T., 1982. Numerical-models for dilute gas-particle flows – review. J. Fluid Eng. 104, 297–303.

Squires, K.D., Eaton, J.K., 1990. Particle response and turbulence modification in isotropic turbulence. Phys. Fluids 2, 1191–1203.

Sundaram, S., Collins, L.R., 1996. Numerical considerations in simulating a turbulent suspension of finite-volume particles. J. Comput. Phys. 124, 337–350.

Snider, D.M., 2001. An incompressible three-dimensional multiphase particle-in-cell model for dense particle flows. J. Comput. Phys. 170 (2), 523–549.

Magnaudet, J., Eames, I., 2000. The motion of high-Reynolds-number bubbles in inhomogeneous flows. Annu. Rev. Fluid Mech. 32, 659–708.

Clift, R., Grace, J.R., Weber, M.E., 1978. Bubbles, Drops, and Particles. Dover Publications.

Parmar, M., Haselbacher, A., Balachandar, S., 2008. On the unsteady inviscid force on cylinders and spheres in subcritical compressible flow. Phil. Trans. R. Soc. A 366, 2161–2175.

Sangani, A.S., Zhang, D.Z., Prosperetti, A., 1991. The added mass, Basset, and viscous drag coefficients in nondilute bubbly liquids undergoing small-amplitude oscillatory motion. Phys. Fluids A 3, 2955.

Ferry, J., Balachandar, S., 2001. A fast Eulerian method for disperse two-phase flow. Int. J. Multiphase Flow 27, 1199–1226.

Ferry, J., Rani, S.L., Balachandar, S., 2003. A locally implicit improvement of the equilibrium Eulerian method. Int. J. Multiphase Flow 29, 869–891.

Mei, R., Adrian, R.J., 1992. Flow past a sphere with an oscillation in the free-stream velocity and unsteady drag at finite Reynolds number. J. Fluid Mech. 237, 323–341.

Balachandar, S., Ha, M.Y., 2001. Unsteady heat transfer from a sphere in a uniform cross-flow. Phys. Fluids 13, 3714–3728.

Bagchi, P., Balachandar, S., 2003. Effect of turbulence on the drag and lift of a particle. Phys. Fluids 15, 3496.

Merle, A., Legendre, D., Magnaudet, J., 2005. Forces on a high-Reynolds-number spherical bubble in a turbulent flow. J. Fluid Mech. 532, 53–62.

Zeng, L., Balachandar, S., Fischer, P., Najjar, F., 2008. Interactions of a stationary finite-sized particle with wall turbulence. J. Fluid Mech. 594, 271–305.

Rudinger, G., 1964. Some properties of shock relaxation in gas flows carrying small particles. Phys. Fluids 7, 658–663.

Ling, Y., Haselbacher, A., Balachandar, S., 2009. Transient phenomena in one-dimensional compressible gas-particle flows. Shock Waves 19, 67–81.

Zhang, F., Thibault, P.A., Link, R., 2003. Shock interaction with solid particles in condensed matter and related momentum transfer. Proc. R. Soc. Lond. A Mat. 459, 705–726.

Parmar, M., Haselbacher, A., Balachandar, S., 2010. Improved drag correlation for spheres and application to shock-tube experiments. AIAA J. 48, 1273–1276.

Longhorn, A.L., 1952. The unsteady, subsonic motion of a sphere in a compressible inviscid fluid. Quart. J. Mech. Appl. Math. 5, 64–81.